ACS Catalysis

RESEARCH ARTICLE

pubs.acs.org/acscatalysis

Enhancement of the Catalytic Activity of Titanium-Based Terminal Olefin Epoxidation Catalysts via Surface Modification with Functionalized Protic Molecules

Paul J. Cordeiro[†,§] and T. Don Tilley[*,‡,§]

[†]Department of Chemical and Biomolecular Engineering and [‡]Department of Chemistry, University of California, Berkeley, Berkeley, California 94720, United States

[§]Chemical Sciences Division, Lawrence Berkeley National Laboratory, 1 Cyclotron Road, Berkeley, California 94720, United States

Supporting Information

ABSTRACT: Site-isolated Ti(IV) centers were introduced onto the surface of a mesoporous SBA-15 support via the thermolytic molecular precursor method. Prior to thermal treatment to generate Ti−OH sites, residual silanol groups were capped via reaction with Me_2N-$SiMe_3$ to give **TiMe$_{cap}$SBA15**. After low temperature treatment in oxygen, the resulting Ti−OH sites of **TiMe$_{cap}$SBA15-O$_2$** were modified by reaction with a series of protic reagents: phenol, pentafluorophenol, acetic acid, and trifluoroacetic acid. The structure of the resulting **TiSBA15** catalysts and the Ti(IV) epoxidation intermediates (formed upon treatment of Ti(IV) materials with TBHP or H_2O_2) were probed using diffuse-reflectance UV−visible spectroscopy and infrared spectroscopy. A titanium-hydroperoxo species similar to that found in TS-1 is proposed for all catalysts. Samples modified with phenol and pentafluorophenol exhibited conversions of 1-octene that are 20 to 50% higher than those for **TiMe$_{cap}$SBA15-O$_2$**, without a significant drop in selectivity for the epoxide product, 1,2-epoxyoctane, when TBHP was used as the oxidant. With aqueous H_2O_2 as the oxidant, the phenol-treated materials exhibited 1-octene conversions that are 15 to 50% greater than those observed for **TiMe$_{cap}$SBA15-O$_2$**, and an increased selectivity for 1,2-epoxyoctane of 10 to 30%. Additionally, the efficiency of H_2O_2 usage, as monitored via ^{1}H NMR spectroscopy, increased by a factor of 2 to three for catalysts modified with phenol and pentafluorophenol, with respect to the efficiency observed over **TiMe$_{cap}$SBA15-O$_2$**. Catalysts modified with acetic acid and trifluoroacetic acid displayed decreased catalytic turnover numbers and epoxide selectivities when TBHP was used as the oxidant, but exhibited catalytic turnover numbers and epoxide selectivities similar to **TiMe$_{cap}$SBA15-O$_2$** when H_2O_2 was used as the oxidant. After treatment of **TiMe$_{cap}$SBA15-O$_2$** with acetic acid, the H_2O_2 efficiency decreased by a factor of 2 for the epoxidation of 1-octene with H_2O_2.

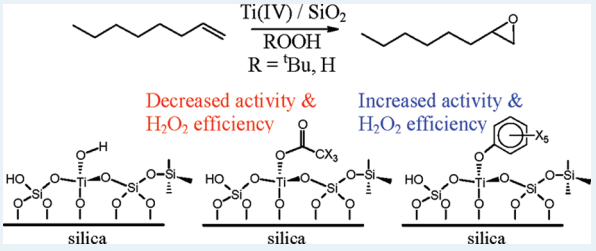

KEYWORDS: epoxidation, hydrogen peroxide, surface modification, titania-silica, titanium-peroxox, single site, molecular precursor

INTRODUCTION

Since the development of a heterogeneous, silica-supported Ti(IV) catalyst by Shell in the 1970s,[1] numerous Ti(IV)-based catalysts have been studied for the direct functionalization of inexpensive and readily available alkanes and alkenes into more synthetically useful molecules such as aldehydes, ketones, and epoxides.[2−6] Particular attention has been paid to supported, site-isolated Ti(IV)/SiO_2 catalysts for selective oxidation reactions, and in particular the epoxidation of olefins. Epoxides are important chemical intermediates in the production of fine chemicals, and products such as propylene oxide are used in polyether polymer synthesis.[7−9] The large-scale industrial production of epoxides in the liquid phase generally involves chlorinated solvents or coreactants, and produces equimolar amounts of coproducts that can be of limited industrial use, difficult to recycle, and/or environmentally harmful. Terminal olefins (e.g., 1-octene) present a greater challenge because of their electron-deficient nature as compared to cyclic olefins (e.g., cyclohexene), while their products are highly desirable as versatile starting materials.[10−12] Many of the known, effective titanium-containing supported catalysts are based on titanium-substituted zeolite frameworks (TS-1, TS-2, Ti-β) with microporous (∼ 6 Å) channels, which restrict their usage to smaller substrates.[13] Thus, catalysts with larger channel diameters based on mesoporous silica frameworks (MCM, SBA) are highly desired.

A well-established technique for the preparation of isolated, single-site transition metal catalysts is based on the thermolytic molecular precursor (TMP) method,[14,15] which employs metal containing species rich in silicon and oxygen (in the form of siloxy and alkoxy ligands) to deliver isolated active sites onto

Received: January 12, 2011
Revised: March 10, 2011
Published: March 15, 2011

Scheme 1. Thermolytic Molecular Precursor Route for the Introduction of Site-Isolated Metal Centers onto Oxide Supports

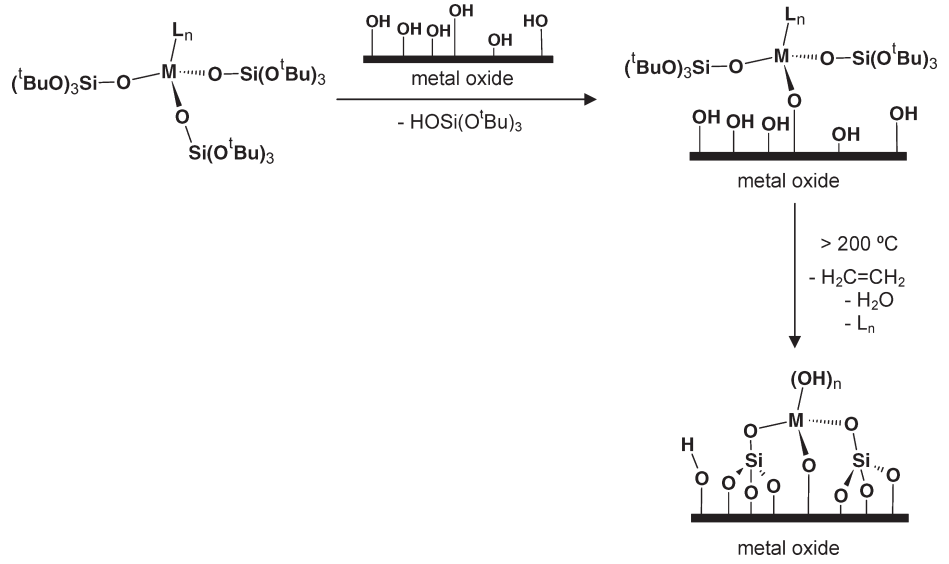

Scheme 2. Proposed Mechanism for Cyclohexene Epoxidation with H_2O_2 and R_{cap}TiSBA15 Catalysts

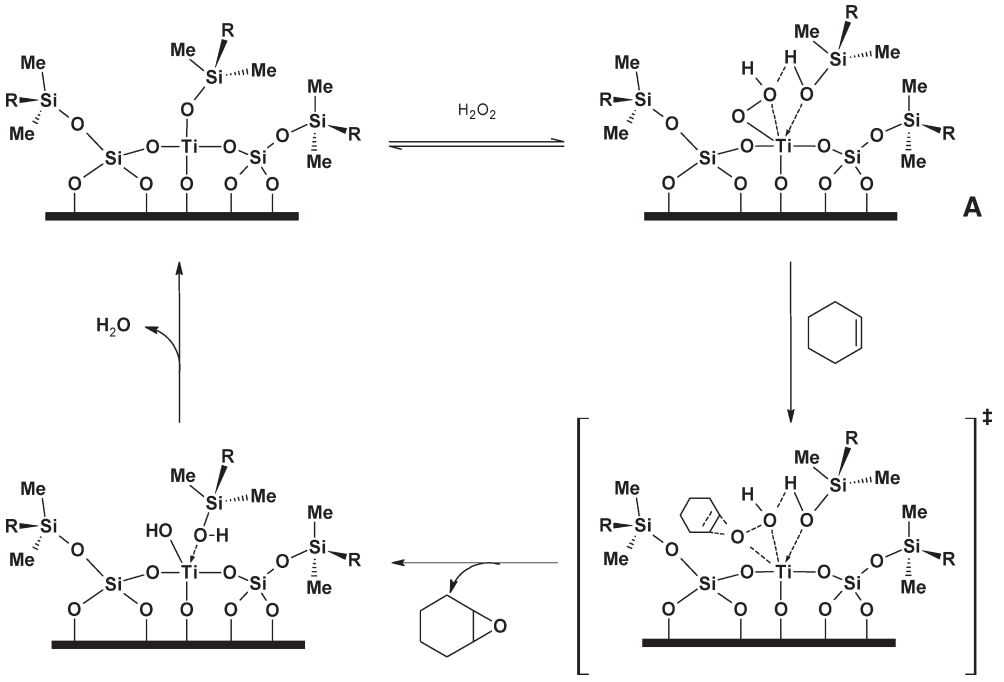

mesoporous supports under mild conditions (Scheme 1). These precursor molecules react with surface silanol (Si−OH) groups via protonolysis reactions to eliminate silanol or alcohol molecules and anchor the metal center to the surface. A mild temperature (<500 K) treatment in oxygen may then be employed to generate metal hydroxide sites (M−OH), which can then be further functionalized. This approach, along with the use of similar molecules, has led to the development of numerous site-isolated catalytic materials displaying improved activity and/or selectivity in the oxidation of hydrocarbons.[16−28]

In general, these materials inherently exhibit drastically lower catalytic activities when aqueous hydrogen peroxide is used as the oxidant in place of alkyl hydroperoxides, such as *tert*-butyl hydroperoxide (TBHP). This poor performance of supported titanium(IV) catalysts in the epoxidation of alkenes (via an electrophilic oxygen transfer) using aqueous H_2O_2 has been attributed to competitive binding of water molecules in place of H_2O_2 and/or deactivation of the active hydroperoxy intermediate.[1,29] Also, many metal-based catalysts catalyze the decomposition of hydrogen peroxide to water and oxygen gas, leading to low catalytic efficiencies for this reagent.[30] Several studies in recent years have addressed these issues with methods for the surface modification of transition metal epoxidation catalysts to generate hydrophobic surfaces and/or influence the structure of the metal

dx.doi.org/10.1021/cs200017s |*ACS Catal.* 2011, 1, 455–467

Scheme 3. Synthesis of TiSBA15, Surface Modification of TiSBA15 to Yield $TiMe_{cap}TaSBA15$, and $TiMe_{cap}SBA15\text{-}O_2$, and Surface Modification of $TiMe_{cap}SBA15\text{-}O_2$ to Yield $X_{cap}TiMe_{cap}SBA15$ (X = Ph, C_6F_5, C(=O)Me, $C(=O)CF_3$)

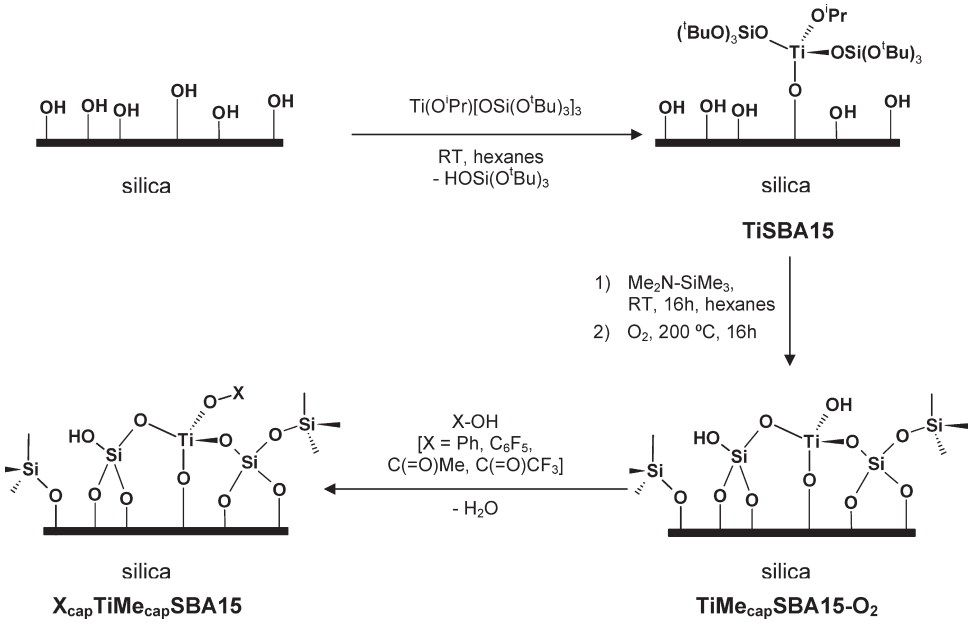

site.[31−34] In particular, the Lewis acidity of the metal center is thought to play an important role in the activity of metal-peroxide active species.[35,36]

The study described here was motivated by recent reports indicating that siloxy groups bound directly to surface-bound, active titanium(IV) centers via a Ti−O−Si linkage may greatly improve catalytic performance for epoxidation.[34,37−41] Such centers, $(SiO_{surface})_3Ti(OSiR_3)$, appear to be more electron deficient and more active for alkene epoxidation compared with the uncapped counterpart, $(SiO_{surface})_3Ti(OH)$, on the basis of theoretical and experimental studies.[38−41] The more electropositive character of the capped titanium center could result in a more facile electrophilic oxygen transfer from the Ti(IV)−OOH intermediate to the olefin (Scheme 2). After the oxygen transfer, the $(SiO_{surface})_3Ti-OH$ unit and the coordinated silanol ($pK_a \sim 13$) molecule likely condense to release H_2O and regenerate the capped titanium center; a related process has been experimentally observed for the epoxidation of ethylene and propylene with H_2O_2 and TS-1.[42]

The importance of hydrogen bonding in metal-based oxidation reactions, specifically with regards to metal-peroxo and metal-hydroperoxo species, has been addressed in several investigations.[43−49] Specifically, hydrogen bonding involving metal-peroxo species has been implicated as a key factor influencing the rate of epoxidation of olefins.[45,46] This type of interaction can activate or deactivate a metal-peroxo species, as demonstrated (for example) by the inactivity of deprotonated titanium-containing polyoxometallates, versus the more active, protonated form.[50,51] A recent report by Berkessel and Adrio detailed the activation of H_2O_2 toward olefin epoxidation through a network of hydrogen-bonding interactions with several molecules of fluorinated alcohol.[43] The study described here was designed to probe such hydrogen bond effects in active centers of type **A** (Scheme 2), by comparing the catalytic performance of surface-bound Ti(IV) sites possessing various Ti−O−R groups (Scheme 3, R = Ph, C_6F_5, C(=O)Me, $C(=O)CF_3$). These groups, which should give rise to Ti(ROH)(OOH) species that may be stabilized by intramolecular hydrogen bonding interactions analogous to that in **A**, are expected to influence the efficiency of catalytic epoxidation reactions. By varying the proton-donor ability of the −OR group, it may be possible to probe the role of this hydrogen-bond interaction in electrophilic oxygen transfer to olefins.

In this study, site-isolated Ti(IV) centers were introduced onto the surface of mesoporous SBA-15 via the thermolytic molecular precursor method.[14,15,52] The resulting materials were characterized by diffuse reflectance UV−visible (DRUV−vis) spectroscopy, infrared spectroscopy, thermogravimetric analysis (TGA), and hydroxyl group titration to probe the coordination environment of the Ti(IV) species. After efficient capping of the surface silanol groups via treatment with $Me_2N\text{-}SiMe_3$ to produce a hydrophobic surface, a subsequent low temperature treatment in oxygen was employed to generate surface Ti−OH sites without decomposition of the $-SiMe_3$ capping groups. These titanol sites were then modified with a series of small protic molecules to generate new, surface-bound Ti−O−R species. The performance of these catalysts in the epoxidation of 1-octene with anhydrous *tert*-butyl hydroperoxide and aqueous hydrogen peroxide was then evaluated.

RESULTS

Synthesis and Characterization of Materials. Mesoporous SBA-15 silica was synthesized according to a literature procedure.[53] Titanium-containing materials were synthesized according to previously reported procedures by grafting $Ti(O^iPr)[OSi(O^tBu)_3]_3$ onto the silica surface to yield **TiSBA15**.[19] After drying under vacuum, these materials were modified with $-SiMe_3$ groups to replace available terminal Si−OH sites, as described previously, by reaction of **TiSBA15** with (*N*,*N*-dimethamino)trimethylsilane

dx.doi.org/10.1021/cs200017s |*ACS Catal.* 2011, 1, 455–467

Table 1. Elemental Analysis, Surface Modification, and Nitrogen Physisorption Data for Dispersed Ti(IV) Materials

material	Ti content [wt %][a]	Ti content [nm^2][a]	−OH content [nm^2][b]	X[c] coverage [nm^{-2}][d]	X/Ti [mol-mol^{-1}]	S_{BET} [m^2 g^{-1}]	r_p[e] [nm]
SBA15			1.0			770	3.3
TiSBA15	1.14	0.18	0.8			410	2.8
TiMe$_{cap}$SBA15	1.00	0.16	0.2	0.6	3.7	330	2.8
TiMe$_{cap}$SBA15-O$_2$	1.00	0.16	0.6			330	2.8
(C$_6$H$_5$)$_{cap}$TiMe$_{cap}$SBA15	0.90	0.15	0.3	0.3	1.7	310	2.8
(C$_6$F$_5$)$_{cap}$TiMe$_{cap}$SBA15	0.90	0.15	0.2	0.4	2.7	300	2.8
(CH$_3$CO)$_{cap}$TiMe$_{cap}$SBA15	0.92	0.15	0.1	0.5	3.3	290	2.8
(CF$_3$CO)$_{cap}$TiMe$_{cap}$SBA15	0.96	0.16	0.2	0.4	2.6	290	2.8

[a] Determined by inductively coupled plasma (ICP) methods. [b] Determined by titration with Mg(CH$_2$C$_6$H$_5$)$_2$·2THF. [c] X − capping group; −SiMe$_3$ (Me), C$_6$H$_5$, C$_6$F$_5$, CH$_3$CO, CF$_3$CO. [d] Determined by carbon elemental analysis, TGA, and titration of residual −OH groups with Mg(CH$_2$C$_6$H$_5$)$_2$·2THF. [e] Pore radius determined from BJH adsorption.

(Me$_2$N-SiMe$_3$)[34] to afford **TiMe$_{cap}$SBA15**. This material was treated in oxygen at 200 °C to decompose the siloxide and alkoxide ligands bound to titanium and generate Ti−OH sites, while leaving the −SiMe$_3$ capping groups intact.[34,37] This treatment provided samples designated as **TiMe$_{cap}$SBA15-O$_2$** (Scheme 3).

The degree of surface functionalization was determined from carbon elemental analysis, TGA, and differences in surface hydroxyl content. The density of surface −OH groups was determined by monitoring reactions of the samples with Mg(CH$_2$Ph)$_2$·2THF, and quantifying the amount of toluene evolved after the reaction via ^{1}H NMR spectroscopy.[54] The extent of surface Si−OH capping by Me$_2$N-SiMe$_3$, measured by titration of the residual hydroxyls with Mg(CH$_2$Ph)$_2$·2THF, resulted in a surface coverage of 0.6 groups per square nanometer (3.7 groups per titanium atom; thus 72% of all Si−OH groups were consumed, as shown in Table 1). Carbon elemental analysis and TGA of **TiSBA15** and **TiMe$_{cap}$SBA15** displayed a large increase in mass attributed to carbon, which when normalized to the mass of the −SiMe$_3$ group, resulted in a similar coverage of −SiMe$_3$ groups per square nanometer. After treatment in oxygen to decompose the organic ligands bound to titanium and generate surface Ti−OH sites, the surface hydroxyl content increased, indicating that more −OH sites were created or became accessible after oxygen treatment. The amount of carbon present in **TiMe$_{cap}$SBA15-O$_2$** also decreased, and this is consistent with an observed increase in the −OH site density, and by an observed reduction in mass during TGA experiments. Diffuse reflectance UV−visible spectroscopy was used to probe the local structure of the titanium centers in these catalysts. Figure 1 presents the DRUV−vis spectra for **TiSBA15**, **TiMe$_{cap}$SBA15**, and **TiMe$_{cap}$-SBA15-O$_2$**. All spectra are dominated by an absorption band centered between 210 and 220 nm, ascribed to a totally symmetric ligand to metal charge transfer from the four neighboring oxygen atoms to the titanium atom (O→Ti), characteristic of site-isolated, tetrahedral titanium centers.[55] Upon surface modification via −SiMe$_3$ groups and subsequent treatment in oxygen, the absorption band broadens, but its maximum remains below 220 nm, and the onset of absorption is below 300 nm.

Infrared spectroscopy was employed to determine if the treatment at 200 °C in oxygen might result in significant decomposition of −SiMe$_3$ groups and regeneration of surface Si−OH sites. Spectra of **TiMe$_{cap}$SBA15** before heat treatment samples exhibited weak intensity bands assigned to a minority of Si−OH groups that were not replaced by −SiMe$_3$ moieties.

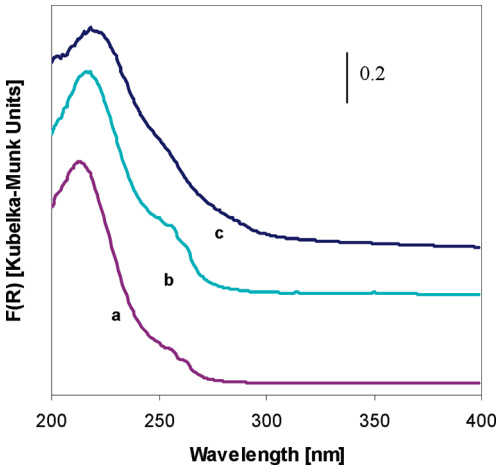

Figure 1. DRUV−vis spectra for (a) **TiSBA15**, (b) **TiMe$_{cap}$SBA15**, and (c) **TiMe$_{cap}$SBA15-O$_2$**. Spectra are offset for clarity.

These spectra were essentially unchanged when the materials were treated in oxygen at low temperature (**TiMe$_{cap}$SBA15-O$_2$**); however, treatment at high temperatures (500 °C) regenerated the Si−OH band to an intensity comparable to those of unmodified **TiSBA15**. Since no Ti−OH sites were identified by FTIR experiments, direct evidence for the presence of Ti−OH sites was obtained using the method reported by Lin and Frei.[56] Briefly, samples of SBA15 and **TiMe$_{cap}$SBA15-O$_2$** were treated with SnCl$_2$·2H$_2$O in an acetonitrile/dichloromethane solution, and then filtered and dried to yield **Sn-SBA15** and **Sn-TiMe$_{cap}$SBA15**. DRUV−vis spectra of both of the resulting materials displayed intense absorptions for tin species centered at 217 nm (Supporting Information, Figure S1A). The spectra of **Sn-TiMe$_{cap}$SBA15** also displayed a shoulder between 250 and 300 nm. This shoulder is absent in the sample without titanium. These spectra and the difference of the two spectra (Supporting Information, Figure S1B) exhibit a shape and energy similar to those reported for Ti−O−Sn and other bimetallic M−O−M′ complexes supported on molecular sieves.[56−60] After treatment with SnCl$_2$·2H$_2$O, the spectrum of **TiMe$_{cap}$SBA15** remained unchanged, and did not exhibit a shoulder between 250 and 300 nm.

Titanium-capped materials **(C$_6$X$_5$)$_{cap}$TiMe$_{cap}$SBA15** and **(CX$_3$CO)$_{cap}$TiMe$_{cap}$SBA15** (X = H, F) were obtained by

dx.doi.org/10.1021/cs200017s |ACS Catal. 2011, 1, 455–467

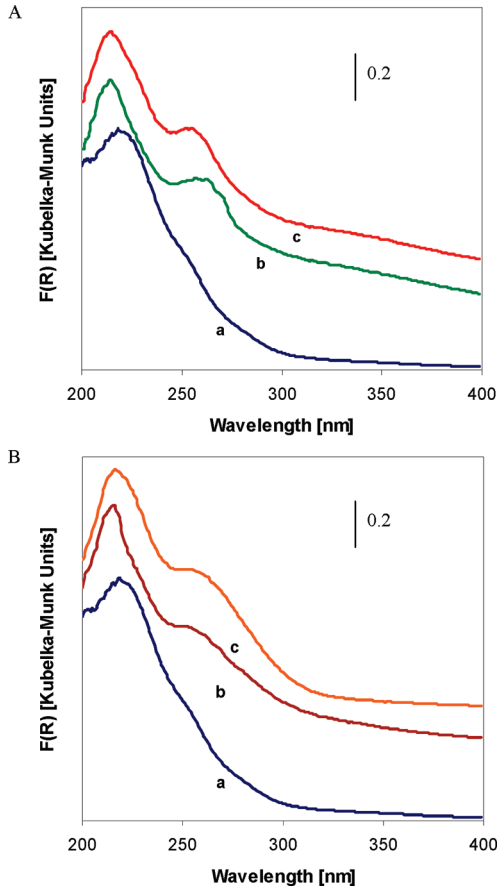

Figure 2. (A) DRUV−vis spectra for (a) $\mathbf{TiMe_{cap}SBA15\text{-}O_2}$, (b) $\mathbf{(C_6H_5)_{cap}TiMe_{cap}SBA15}$, and (c) $\mathbf{(C_6F_5)_{cap}TiMe_{cap}SBA15}$. (B) DR-UV−vis spectra for (a) $\mathbf{TiMe_{cap}SBA15\text{-}O_2}$, (b) $\mathbf{(CH_3CO)_{cap}TiMe_{cap}SBA15}$, and (c) $\mathbf{(CF_3CO)_{cap}TiMe_{cap}SBA15}$. Spectra are offset for clarity.

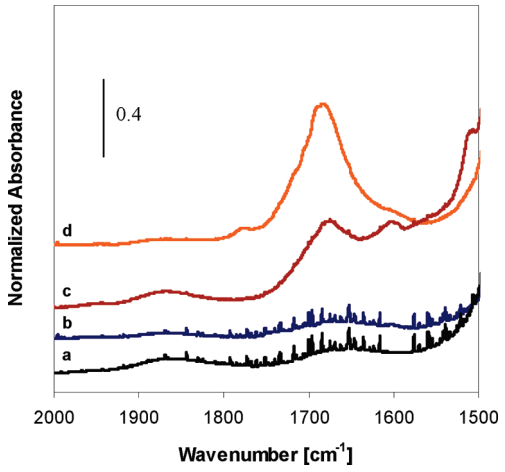

Figure 3. Room temperature FTIR spectra for (a) SBA15, (b) $\mathbf{TiMe_{cap}SBA15\text{-}O_2}$, (c) $\mathbf{(CH_3CO)_{cap}TiMe_{cap}SBA15}$, and (d) $\mathbf{(CF_3CO)_{cap}TiMe_{cap}SBA15}$. Spectra are offset for clarity.

treatment of $\mathbf{TiMe_{cap}SBA15\text{-}O_2}$ with the appropriate protic compound (C_6X_5OH or CX_3COOH, X = H, F) at 65 °C in toluene to titrate the Ti−OH sites (Scheme 3). After washing with toluene, these samples were filtered and dried at 120 °C under vacuum. Solution state ^{1}H NMR spectra of the filtrate displayed resonances characteristic of water, the expected product of the reaction of these molecules with surface Ti−OH sites. Direct evidence for the presence of the individual, secondary capping groups on the surface was obtained via DRUV−vis and infrared spectroscopies. DRUV−vis spectra of the capped materials retained the intense absorption centered between 210 and 220 nm due to the symmetric O→Ti ligand-to-metal charge transfer (LMCT),[55] but also exhibited new features between 250 and 400 nm. In the case of $\mathbf{(C_6X_5)_{cap}TiMe_{cap}SBA15}$ (X = H, F), these transitions arise from phenol $\pi-\pi^*$ transitions (Figure 2A), and can also be observed in spectra of SBA-15 treated with phenol or pentafluorophenol (Supporting Information, Figure S2), and solution state spectra of these molecules. Similarly, the spectra of $\mathbf{(CX_3CO)_{cap}TiMe_{cap}SBA15}$ (X = H, F) and SBA-15 treated with acetic acid or trifluoroacetic acid displayed new absorption bands below 400 nm (Figure 2B, Supporting Information, Figure S2) similar to those observed for acetic acid and trifluoro acetic acid in the solution state. It should be noted that these bands are present regardless of solvent choice, and are not due to residual toluene solvent present in the system.[61] Additionally, infrared spectra of $\mathbf{(CX_3CO)_{cap}TiMe_{cap}SBA15}$ (X = H, F) exhibited new bands between 1600 and 1750 cm^{-1}, due to carboxylic acid carbonyl stretches (Figure 3). The carbonyl band for $\mathbf{(CH_3CO)_{cap}TiMe_{cap}SBA15}$ appeared at 1675 cm^{-1}, at a slightly lower energy than the band for $\mathbf{(CF_3CO)_{cap}TiMe_{cap}SBA15}$ at 1685 cm^{-1}. These bands are distinct from those associated with free acetic acid (1715 cm^{-1}) and trifluoroacetic acid (1783 cm^{-1}). The shift of the frequency of the C═O band to lower energy is consistent with bands observed for $Cp_2Ti[CO_2CF_3]_2$ (1710 cm^{-1}),[62] $Cp_2Ti[OC(=O)^tBu]X$ (1636−1645 cm^{-1}, X = $OC(=O)^tBu$, $OC(=O)Ph$, $OTi(Cp_2)(OC(=O)^tBu)$, and $OC(=O)^tBu$),[63] and other transition metal perfluorocarboxylate derivatives.[62] No bands due to C−F stretches could be observed in spectra of both $\mathbf{(CF_3CO)_{cap}TiMe_{cap}SBA15}$ and $\mathbf{(C_6F_5)_{cap}TiMe_{cap}SBA15}$.

Quantification of the number of secondary capping groups present on the surface was determined from carbon elemental analysis, TGA, and differences in surface hydroxyl content. All modified catalysts ($\mathbf{X_{cap}TiMe_{cap}SBA15}$, X = Ph, C_6F_5, C(═O)Me, $C(=O)CF_3$) exhibited decreased surface hydroxyl content compared to $\mathbf{TiMe_{cap}SBA15\text{-}O_2}$, as measured by titration with $Mg(CH_2Ph)_2\cdot 2THF$, though a minority of hydroxyls remained unreacted in all capped samples. TGA of the modified samples (containing secondary capping groups) demonstrated an increased mass loss compared to $\mathbf{TiMe_{cap}SBA15\text{-}O_2}$, which, when normalized to the molecular weight of the capping group, correlated well with the number of hydroxyl groups that reacted with protic capping groups, determined via titration with $Mg(CH_2Ph)_2\cdot 2THF$. This was also confirmed by the increased amount of carbon present in modified samples compared to $\mathbf{TiMe_{cap}SBA15\text{-}O_2}$, measured by elemental analysis. The capping efficiencies for all samples were roughly equivalent, with between 0.3 and 0.5 groups per square nanometer, corresponding to between 1.7 and 3.3 groups per titanium atom (Table 1). These numbers are larger than unity perhaps because of the presence of a minority of residual silanol sites remaining after titration with $Me_2N\text{-}SiMe_3$, which are also able to react with the protic molecules used in this study, or because of a small amount of leaching of titanium (though the titanium content remained close to the value determined for $\mathbf{TiMe_{cap}SBA15\text{-}O_2}$; Table 1).

The surface areas and pore structures of the materials were evaluated using nitrogen porosimetry. All samples displayed N_2

dx.doi.org/10.1021/cs200017s |ACS Catal. 2011, 1, 455–467

Table 2. Thermal Analysis (to 150 °C) of Dispersed Ti(IV) Catalysts after Hydration for 48 h[a]

material	H_2O content (wt %)[a]	desorption temperature (°C)[b]
SBA15	38.0	63
TiSBA15	34.1	77
$TiMe_{cap}SBA15$	5.5	52
$TiMe_{cap}SBA15\text{-}O_2$	12.2	57
$(C_6H_5)_{cap}TiMe_{cap}SBA15$	4.3	45
$(C_6F_5)_{cap}TiMe_{cap}SBA15$	17.9	44
$(CH_3CO)_{cap}TiMe_{cap}SBA15$	21.7	73
$(CF_3CO)_{cap}TiMe_{cap}SBA15$	46.5	83

[a] Samples were stored in a sealed container with a saturated water environment. [b] The minimum of endothermic transition for water loss determined by DSC.

adsorption−desorption data consistent with type IV isotherms (Supporting Information, Figure S3), with narrow pore size distributions, characteristic of SBA15 type materials.[53] The unmodified **TiSBA15** catalyst was found to have a Brunauer−Emmet−Teller (BET) surface area of 410 $m^2\ g^{-1}$. The surface area decreased with surface modification, with **$TiMe_{cap}$SBA15** and **$TiMe_{cap}SBA15\text{-}O_2$** both having a surface area of 330 $m^2\ g^{-1}$, and again after modification with phenol or carboxylic acid derivatives (down to 300−310 $m^2\ g^{-1}$, and 290 $m^2\ g^{-1}$ respectively). The pore size distribution for all modified **$X_{cap}TiMe_{cap}SBA15$** catalysts was found to be similar to that of the parent **TiSBA15** (Table 1). The well-ordered mesostructure of all **TiSBA15** catalysts was preserved, as indicated by transmission electron microscopy (TEM) and by the retention of the low angle reflections in the small-angle X-ray scattering (SAXS) patterns (Supporting Information, Figures S4 and S5). The amount of titanium present in each sample was determined by inductively coupled plasma (ICP) optical emission spectroscopy, with a maximum titanium content of 1.14 wt % Ti found for **TiSBA15** (Table 1).

Hydrophobicity of Surface-Modified Materials. To study the hygroscopic nature of the materials, samples were placed in a sealed container with a saturated water atmosphere for 48 h, followed by TGA and differential scanning calorimetry (DSC) analysis (Table 2). Typically, mass lost below 150 °C corresponds to physisorbed water molecules, since fully dehydrated samples display little mass loss until temperatures above 250 °C.[32] This higher temperature mass loss corresponds to the loss of surface $-SiMe_3$ groups, as well as phenol and acetic acid-type capping groups. The water desorption temperature was taken as the minimum of the endothermic transition corresponding to water loss. The unmodified **TiSBA15** displayed a mass loss of 34 wt % and a desorption temperature of 77 °C, similar to unmodified, bare SBA15. These values decrease upon grafting $-SiMe_3$ groups on the surface to 5.5 wt % and 52 °C (**$TiMe_{cap}$SBA15**), and then increase slightly upon oxygen treatment to 12.2 wt % and 57 °C (**$TiMe_{cap}SBA15\text{-}O_2$**), confirming the hydrophobic nature of the materials after surface modification and oxygen treatment. Catalyst samples modified with phenol-type capping groups displayed decreased water desorption temperatures and varied H_2O loss below 150 °C. **$(C_6H_5)_{cap}TiMe_{cap}SBA15$** exhibited a low mass loss (4.3 wt %) and a moderately decreased water desorption temperature (45 °C), while **$(C_6F_5)_{cap}TiMe_{cap}SBA15$** had an increased mass loss

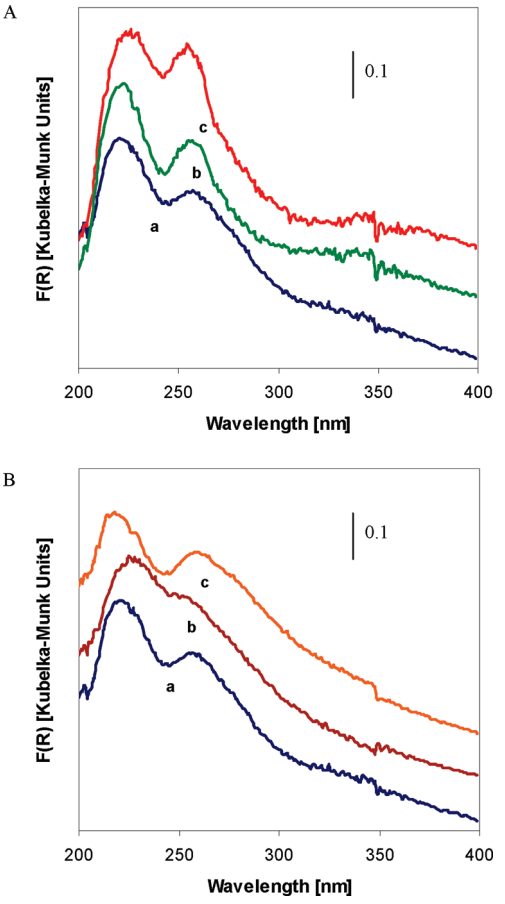

Figure 4. (A) DRUV−vis spectra of samples treated with H_2O_2: (a) **$TiMe_{cap}SBA15\text{-}O_2$**, (b) **$(C_6H_5)_{cap}TiMe_{cap}SBA15$**, and (c) **$(C_6F_5)_{cap}TiMe_{cap}SBA15$**. (B) (B) DRUV−vis spectra of samples treated with H_2O_2: (a) **$TiMe_{cap}SBA15\text{-}O_2$**, (b) **$(CH_3CO)_{cap}TiMe_{cap}SBA15$**, and (c) **$(CF_3CO)_{cap}TiMe_{cap}SBA15$**. Spectra are offset for clarity.

(17.9 wt %), and a similarly decreased desorption temperature (44 °C). In contrast, acetate and trifluoroacetate capping groups significantly decreased the hydrophobicity of the catalyst surface, leading to increased mass loss (21.7 wt % and 46.5 wt % for **$CH_3CO_{cap}TiMe_{cap}SBA15$** and **$CF_3CO_{cap}TiMe_{cap}SBA15$**, respectively) and increased desorption temperatures (73 and 83 °C, respectively). In both types of capped catalyst, the fluorinated capping group led to a more hydrophilic surface (increased mass loss) but no additional decrease in the water desorption temperature.

Observation of Titanium-peroxo Intermediates. Recent work with related supported titanium and tantalum catalysts identified catalytically active hydroperoxo (titanium) and peroxo (tantalum) intermediates with DRUV−vis spectroscopy and infrared spectroscopy.[34,64] These intermediates were formed when Ti(IV) and Ta(V) catalysts were treated with aqueous hydrogen peroxide in the absence of olefin. In the same manner, samples were treated with a 1:1 solution of 30 wt % H_2O_2 and acetonitrile, heated at 65 °C for 1 h (with stirring), cooled, and dried under vacuum for 16 h. The LMCT (O→Ti) band in spectra of all samples was red-shifted by about 5−10 nm, and an additional absorption band centered at 260 nm appeared as a broad shoulder on the original LMCT band (Figure 4). This band was not present in samples without titanium, or in samples

dx.doi.org/10.1021/cs200017s |ACS Catal. 2011, 1, 455–467

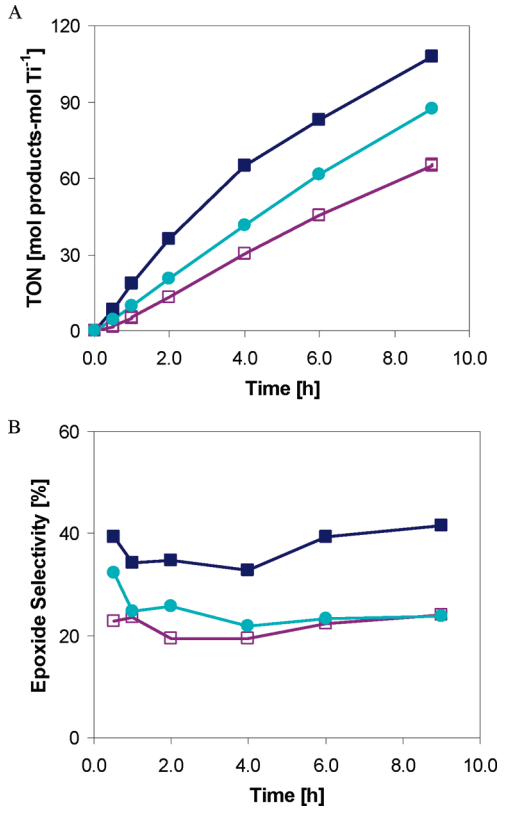

Figure 5. (A) Catalytic TON as a function of time during 1-octene epoxidation reactions with *tert*-butyl hydroperoxide oxidant for **TiSBA15** (□), **TiMe$_{cap}$SBA15** (●), and **TiMe$_{cap}$SBA15-O$_2$** (■). TON = moles of 1-octene oxidation products per mole of titanium(IV). The selectivity to 1,2-epoxyoctane remained greater than 90% at all times. (B) 1,2-epoxyoctane selectivity as a function of time during 1-octene oxidation with reactions with aqueous hydrogen peroxide (30 wt %) for **TiSBA15** (□), **TiMe$_{cap}$SBA15** (●), and **TiMe$_{cap}$SBA15-O$_2$** (■).

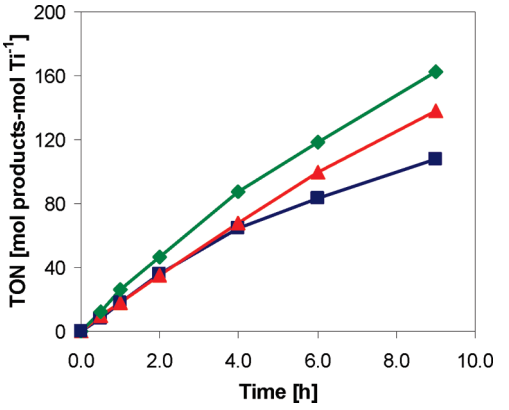

Figure 6. Catalytic TON as a function of time during 1-octene oxidation reactions with *tert*-butyl hydroperoxide oxidant for **TiMe$_{cap}$SBA15-O$_2$** (■), **(C$_6$H$_5$)$_{cap}$TiMe$_{cap}$SBA15** (♦), and **(C$_6$F$_5$)$_{cap}$TiMe$_{cap}$SBA15** (▲). TON = moles of 1-octene oxidation products per mole of titanium(IV).

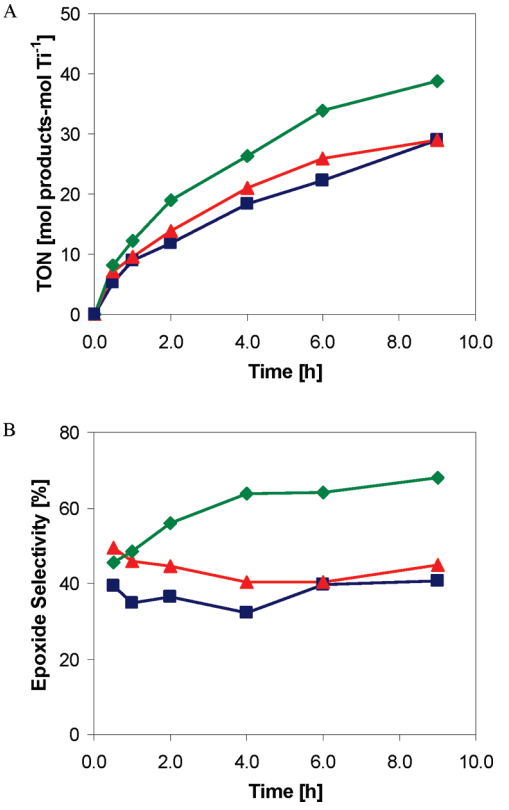

Figure 7. (A) Catalytic TON as a function of time during 1-octene oxidation with H_2O_2 for **TiMe$_{cap}$SBA15-O$_2$** (■), **(C$_6$H$_5$)$_{cap}$TiMe$_{cap}$SBA15** (♦), and **(C$_6$F$_5$)$_{cap}$TiMe$_{cap}$SBA15** (▲). TON = moles of 1-octene oxidation products per mole of titanium(IV). (B) 1,2-epoxyoctane selectivity as a function of time during 1-octene oxidation with H_2O_2 for **TiMe$_{cap}$SBA15-O$_2$** (■), **(C$_6$H$_5$)$_{cap}$TiMe$_{cap}$SBA15** (♦), and **(C$_6$F$_5$)$_{cap}$TiMe$_{cap}$SBA15** (▲).

treated with H_2O in place of aqueous H_2O_2, indicating that both titanium and hydrogen peroxide are required to form the species responsible for the new band. In all peroxide treated samples, this new band can be removed via treatment with a solution of cyclohexene and acetonitrile at 65 °C for 1 h. After cooling, aliquots from these solutions contained significant amounts of oxidation products (measured by gas chromatography), and the DRUV−vis spectra resembled the original, untreated ones (not shown). Samples treated with a 1:1 solution of toluene and *tert*-butyl hydroperoxide displayed identical spectra to those treated with aqueous H_2O_2. Infrared spectra also exhibited a broad band between 3200 cm^{-1} and 3600 cm^{-1}, which has previously been ascribed to a titanium hydroperoxo intermediate.[34,42]

Catalytic 1-Octene Epoxidation. In control experiments with an oxidant and no catalyst (or bare SBA-15), or with a catalyst and no oxidant, no oxidation products of 1-octene were detected by gas chromatography (GC) analysis. Previous reports from this laboratory demonstrated that these types of titanium-based catalysts do not significantly leach under the reaction conditions chosen.[19,34] Additionally, ^{1}H and ^{19}F NMR spectra of aliquots taken during catalytic reactions contained no resonances associated with the capping agents used in this study (C_6X_5 and CX_3CO, X = H, F).

Of the three materials not modified by protic molecules (**TiSBA15**, **TiMe$_{cap}$SBA15**, and **TiMe$_{cap}$SBA15-O$_2$**), **TiMe$_{cap}$SBA15-O$_2$** displayed the highest catalytic turnover number (TON, moles of product per mole of titanium) in the epoxidation of 1-octene with anhydrous *tert*-butyl hydroperoxide (Figure 5A). The selectivity for 1,2-epoxyoctane (the epoxide product) for these catalysts remained essentially the same and was greater than 90%

dx.doi.org/10.1021/cs200017s |*ACS Catal.* 2011, 1, 455–467

Table 3. Catalytic 1-Octene Oxidation with *tert*-Butyl Hydroperoxide for $(CX_3CO)_{cap}TiMe_{cap}SBA15$ (X = H, F) Catalysts[a]

material	time [h]	TON[b]	epoxide selectivity [%]
$TiMe_{cap}SBA15\text{-}O_2$	2	36	97
	6	82	99
	9	107	99
	24	167	>99
$(CH_3CO)_{cap}TiMe_{cap}SBA15$	2	22	80
	6	57	93
	9	71	94
	24	150	97
$(CF_3CO)_{cap}TiMe_{cap}SBA15$	2	25	63
	6	57	79
	9	63	92
	24	123	88

[a] Reaction conditions: 35 mg catalyst, 65 °C, 5 mL of solvent (toluene), 1.55 mL of 1-octene, 1.1 mL of *tert*-butyl hydroperoxide (5.5 M in decane) oxidant, 50 μL standard (dodecane). [b] TON = mol oxidation products/mol Ti.

over a 9 h period. All three catalysts exhibited nearly identical TONs when the oxidant was changed to aqueous H_2O_2 (not shown). However, $TiMe_{cap}SBA15\text{-}O_2$ displayed the highest selectivity to the epoxide (nearly 40% over a 9 h period), while the other two samples displayed epoxide selectivities near 20% (Figure 5B).

Figure 6 depicts the catalytic TON as a function of time for the phenol-capped catalysts with $TiMe_{cap}SBA15\text{-}O_2$, the most active of the uncapped materials, included for reference. The modified materials exhibited an increased conversion of 1-octene, with $(C_6H_5)_{cap}TiMe_{cap}SBA15$ displaying a 50% increase over the uncapped material at all times, and $(C_6F_5)_{cap}TiMe_{cap}SBA15$ displaying a 20% increase in TON at longer times, with TBHP used as an oxidant. This increase occurred without a significant loss in epoxide selectivity (80% after 0.5 h, and greater than 90% after 1 h). These materials also exhibited increased performance with aqueous H_2O_2 as an oxidant (Figure 7). The phenol capped sample, $(C_6H_5)_{cap}TiMe_{cap}SBA15$, displayed a 50% increase in TON compared to $TiMe_{cap}SBA15\text{-}O_2$, and a significant improvement in epoxide selectivity, reaching 56% after 2 h and rising to 68% after 9 h. The fluorinated counterpart, $(C_6F_5)_{cap}TiMe_{cap}SBA15$, exhibited a 15% improvement in TON, and epoxide selectivity was increased to roughly 50% during the reaction. Both samples are associated with a significantly increased efficiency of H_2O_2 (moles of product(s) per mole of H_2O_2 consumed) during the reaction, doubling or tripling the efficiency displayed by the uncapped $TiMe_{cap}SBA15\text{-}O_2$ catalyst (Table 5).

In contrast, carboxylic acid surface additives decreased the catalytic TON (a nearly 30−40% decrease observed over 24 h of reaction) when TBHP was used as the oxidant (Table 3). The epoxide selectivity also decreased during short times, and then rose during the course of the reaction, just below the level exhibited by $TiMe_{cap}SBA15\text{-}O_2$ (90−95% vs 95%). When H_2O_2 was used as the oxidant, the acetic acid-treated materials displayed a TON similar to that for $TiMe_{cap}SBA15\text{-}O_2$ (~10% change), and $(CF_3CO)_{cap}TiMe_{cap}SBA15$ displayed an increase in epoxide selectivity (~ 60% vs 40%), while the selectivity with $(CH_3CO)_{cap}TiMe_{cap}SBA15$ remained essentially unchanged

Table 4. Catalytic 1-Octene Oxidation with H_2O_2 for $(CX_3CO)_{cap}TiMe_{cap}SBA15$ (X = H, F) Catalysts[a]

material	time [h]	TON[b]	epoxide selectivity [%]
$TiMe_{cap}SBA15\text{-}O_2$	2	12	37
	6	22	40
	9	29	41
	24	46	45
$(CH_3CO)_{cap}TiMe_{cap}SBA15$	2	11	38
	6	19	39
	9	24	38
	24	52	49
$(CF_3CO)_{cap}TiMe_{cap}SBA15$	2	13	71
	6	21	62
	9	27	58
	24	49	59

[a] Reaction conditions: 35 mg catalyst, 65 °C, 5 mL of solvent (CH_3CN), 1.55 mL of 1-octene, 0.62 mL of H_2O_2 (30 wt % in H_2O) oxidant, 25 μL standard (toluene). [b] TON = mol oxidation products/mol Ti.

(Table 4). Both of these materials exhibited a decreased H_2O_2 efficiency to approximately 50% of that associated with $TiMe_{cap}SBA15\text{-}O_2$ (Table 5). It should be noted that ^1H and ^{19}F NMR spectra of aliquots taken during the reaction did not exhibit any evidence for leaching of the capping groups. In all cases when H_2O_2 was used as the oxidant, small amounts (~3−5% selectivity) of 1,2-octanediol (the acid catalyzed ring-opening product) were observed.

DISCUSSION

Synthesis and Characterization of Ti(IV) Catalysts. Treatment of the silica surface with $Me_2N\text{-}SiMe_3$ anchors the Me_3Si group to a surface oxygen atom, liberating $HNMe_2$ (detected by ^1H NMR spectroscopy) as has been previously reported.[34] Subsequent low temperature treatment in oxygen decomposes the organic ligands on titanium, to generate Ti−OH sites, while keeping the $-SiMe_3$ groups intact.[34,65] The presence of Ti−OH sites was probed using the method of Lin and Frei, employing $SnCl_2$. The spectrum of $Sn\text{-}TiMe_{cap}SBA15$ was dominated by the absorption due to tin, which lies on top of the LMCT band for oxygen to titanium, but also contained an additional absorption extending out to 400 nm. This type of absorption has previously been attributed to a metal-to-metal charge transfer from titanium to tin ($Ti^{IV}/Sn^{II} \rightarrow Ti^{III}/Sn^{III}$).[56] The spectrum of $TiMe_{cap}SBA15$ remained unchanged after an analogous treatment with $SnCl_2$, indicating that an equivalent Ti−Sn metal-to-metal charge transfer complex is not formed in this sample. This suggests that the low temperature treatment in oxygen removes the organic protecting groups bound to titanium, and is strong evidence for the presence and availability of Ti−OH sites. Further reaction of the newly generated Ti−OH sites with acidic capping groups releases H_2O (detectable by ^1H NMR spectroscopy), anchoring the new capping group onto the surface. These types of reactions have previously been reported for similar supported Ti(IV) catalysts.[35,36,66] These mild, low temperature treatments do not disturb the mesoporous framework, as demonstrated by the type-IV isotherm obtained for all surface modified samples, and by retention of the low angle reflection in the small-angle X-ray scattering patterns.

dx.doi.org/10.1021/cs200017s |ACS Catal. 2011, 1, 455–467

Table 5. Hydrogen Peroxide Efficiencies in the Oxidation of 1-Octene with Modified TiSBA15 Samples $(C_6X_5)_{cap}TiMe_{cap}SBA15$ and $(CX_3CO)_{cap}TiMe_{cap}SBA15$ (X = H, F)[a,b]

	hydrogen peroxide efficiency [%]					
	2 h		6 h		24 h	
catalyst	oxidation products[c]	epoxide	oxidation products[c]	epoxide	oxidation products[c]	epoxide
TiSBA15	2.0	0.4	2.7	0.6	4.5	1.3
$TiMe_{cap}SBA15$	2.7	0.6	5.3	1.3	4.8	1.5
$TiMe_{cap}SBA15\text{-}O_2$	6.2	2.1	7.9	3.1	14.3	6.2
$(C_6H_5)_{cap}TiMe_{cap}SBA15$	12.1	6.7	13.6	9.0	18.2	12.4
$(C_6F_5)_{cap}TiMe_{cap}SBA15$	14.2	6.6	11.2	5.0	10.3	5.2
$(CH_3CO)_{cap}TiMe_{cap}SBA15$	3.5	1.6	3.0	1.3	6.3	2.9
$(CF_3CO)_{cap}TiMe_{cap}SBA15$	2.5	1.7	2.8	1.8	4.5	2.5

[a] Residual peroxide concentrations measured by ^{1}H NMR. [b] Reaction conditions: 35 mg catalyst, 65 °C, 5 mL of CH_3CN, 1.55 mL of 1-octene, 0.62 mL of H_2O_2 (30 wt % in H2O) oxidant, 25 μL toluene (internal standard). [c] Oxidation products: 1,2-epoxyoctane, 1,2-octanediol, 1-octen-3-ol, 1-octen-3-one.

Techniques such as solution UV−visible absorbance spectroscopy, solid-state DRUV−vis spectroscopy, and infrared spectroscopy can be employed to probe the local structure of supported metal sites because of the sensitivity of the LMCT band to metal coordination (UV−vis and DRUV−vis), and the appearance of metal−oxygen and carbon−oxygen stretches (FTIR). The DRUV−vis spectra of all supported Ti(IV) samples are dominated by a high energy LMCT band centered between 210 and 220 nm. This type of absorption is characteristic of an isolated, tetrahedral environment.[67,68] No evidence for larger titanium-oxide domains was observed for any sample via transmission electron microscopy or by X-ray diffraction. The absorption maxima for **$TiMe_{cap}SBA15$** and **$TiMe_{cap}SBA15\text{-}O_2$** shift by about 5 nm, and the absorption band broadens, implying a larger distribution of titanium environments in these materials, a phenomenon that was observed previously with this molecular precursor.[19] However, the major absorptions for these materials still lie below 230 nm, indicating that most of the titanium continues to reside in an isolated, tetrahedral environment.[69] No bands corresponding to Ti−OH and Ti═O stretching vibrations were observed in FTIR spectroscopic analyses. DRUV−vis spectra for **$(C_6X_5)_{cap}TiMe_{cap}SBA15$** and **$(CX_3CO)_{cap}TiMe_{cap}SBA15$** (X = H, F) displayed new absorption bands that appeared as shoulders in the 240 to 350 nm range. In the case of **$(C_6X_5)_{cap}TiMe_{cap}SBA15$** (X = H, F), the shoulder is indicative of $\pi-\pi^*$ transitions of the phenolic capping group, which is also seen in spectra of SBA-15 treated with phenol or pentaflorophenol. However, spectra of samples without titanium do not include the long trailing absorption extending out to 400 nm, which is likely the result of the new Ti−O−X linkage. Infrared spectra of **$(CX_3CO)_{cap}TiMe_{cap}SBA15$** (X = H, F) exhibited bands associated with carbonyl stretches at 1675 cm^{-1} (X = H) and 1685 cm^{-1} (X = F), confirming the presence of these groups on the surface, since the bands for the free acids appear at 1715 cm^{-1} (X = H) and 1783 cm^{-1} (X = F).

Observation of Ti−OOH Intermediates. Numerous studies have been devoted to elucidation of the active species present in Ti(IV) epoxidation catalysts.[5,29,38−42,44,70] Both titanium-peroxo (Ti−OO) and titanium-hydroperoxo (Ti−OOH) species have been proposed. Several molecular examples of titanium-peroxo species have been observed and characterized.[50,71−74] However, it is generally accepted that these species are inactive in the epoxidation of alkenes, in contrast to other transition metal peroxo species of Ta, Mo, and Re, among others.[5,50,51,64,75−78] No molecular titanium-hydroperoxo species have been successfully isolated and characterized to specifically observe the hydroperoxo moiety. Previous spectroscopic studies in this laboratory have identified a Ti−OOH intermediate in the epoxidation of alkenes with H_2O_2.[34,37] Spectroscopic identification of this intermediate was made via the similarity of the DRUV−visible absorption spectrum and infrared spectrum of the solid catalyst with other known Ti−OOH species that are active for alkene epoxidation, such as that in the titanosilicate TS-1.[29,42]

Upon treatment in H_2O_2, the LMCT band in the DRUV−vis spectra of **$TiMe_{cap}SBA15\text{-}O_2$** is red-shifted from the parent O→Ti LMCT band for this sample, and a broad shoulder at about 260 nm trailing to 375 nm develops. This matches the previous report of surface modified Ti(IV) catalysts, suggesting that surface modification prior to treatment in oxygen does not remove the ability for the titanium atoms to interact with H_2O_2. Upon addition of H_2O_2, the main LMCT band of the DRUV spectra of both **$(C_6X_5)_{cap}TiMe_{cap}SBA15$** and **$(CX_3CO)_{cap}TiMe_{cap}SBA15$** (X = H, F) appears red-shifted from the untreated material, and a broad shoulder in the same region as **$TiMe_{cap}SBA15$** is observed. The Ti−OOH stretch also becomes visible in FTIR spectra for treated samples as a broad band centered near 3450 cm^{-1}, as has been previously observed.[34] This suggests that a similar titanium-hydroperoxo species is present in all capped materials. It should be noted that this new band is blue-shifted from the band observed for H_2O_2-treated TS-1 (ca. 400 nm),[29] and further study of this system including Raman and/or X-ray absorption spectroscopies should be conducted to determine what specific differences exist between the two systems. The new DRUV−vis band is also removed upon treatment of the Ti(IV)/H_2O_2 catalysts with an alkene, which produces oxidation products and provides further evidence that this is indeed an active intermediate in the epoxidation of alkenes.

Catalytic Performance. All titanium-containing materials are active for the epoxidation of 1-octene. The initial capping of surface silanol groups led to an increase in alkene epoxidation rate and increased epoxide selectivity with either oxidant used, as has been observed for several other supported Ti(IV) systems.[32,34,79,80] This seems at least partly because of the increase in surface hydrophobicity (seen in the smaller amount of adsorbed water and lower desorption temperature), which

dx.doi.org/10.1021/cs200017s |ACS Catal. 2011, 1, 455–467

suppresses coordination of polar products (epoxide, diol) and the epoxidation byproduct (*tert*-butanol and water) to the Ti(IV) species on the surface. Thermal treatment in oxygen may ease the steric congestion around the active centers, caused by the surrounding bulky $-OSi(O^tBu)_3$ ligands, and allow oxidant and substrate molecules to access the Ti(IV) atoms more readily. Surface hydrophobicity also plays a role in increasing the H_2O_2 efficiency, as observed with related Ta(V) catalysts.[64]

The increased activity exhibited by $(C_6X_5)_{cap}$**TiMe**$_{cap}$**SBA15** (X = H, F) catalysts is consistent with previous reports that describe the capping surface Ti−OH and Si−OH species with a variety of groups. These include replacement of the hydrogen atom with species such as $-SiR_3$, $-SO_2(OH)$, calixarene-based molecules, O−C(R)-C(R′)-O, and *n*-C_8H_{17}-C(H)(O)-CH_2O (the latter two with two bonds to Ti through the two oxygen atoms).[33−36,66,80−82] Theoretical calculations suggest that active sites which are more electron deficient are more reactive toward oxygen transfer to the olefin.[38] Additionally, active sites derived from capped titanium (Ti−OR) species are predicted to be more electropositive and more selective than those derived from uncapped (Ti−OH) groups, based on X-ray absorption studies and theoretical calculations.[38−41] Phenoxide-based ligands have also been shown to partially delocalize charge into the six-membered ring, leading to more electropositive metal centers.[83] DRUV−vis and FTIR spectra of both samples suggest that a similar intermediate is formed for all new catalytic species. The poorer performance of $(C_6F_5)_{cap}$**TiMe**$_{cap}$**SBA15**, which would, in theory, provide an additional electron withdrawing substituent bound to titanium, can perhaps be ascribed to the small decrease in surface hydrophobicity (∼ 13 wt % more adsorbed H_2O) compared to $(C_6H_5)_{cap}$**TiMe**$_{cap}$**SBA15**.

The decreased activity exhibited by $(CX_3CO)_{cap}$**TiMe**$_{cap}$**SBA15** (X = H, F) is also consistent with a decreased surface hydrophobicity, allowing for the coordination of water and polar products to the Ti(IV) centers on the surface. Additionally, the proximity of the carbonyl moiety of the acetic acid capping group could allow for donation of electron density from the oxygen atom to the Ti(IV) center. This would in turn increase the electron density of the metal center, and diminish the apparent electron-withdrawing effect of titanium, leading to a species less active for electrophilic oxygen atom transfer in the active Ti(IV)-hydroperoxo species. A similar situation was reported for isolated Ti(IV)-calixarene molecules with pendant aldehyde groups in close proximity to the Ti(IV) atom.[82] These effects do not prevent the formation of the active titanium hydroperoxo (Ti−OOH) species, as observed by DRUV−vis and FTIR studies. The higher amount of ring-opening products observed for these catalysts is also consistent with an increased polarity of the surface as compared to **TiMe**$_{cap}$**SBA15-O**$_2$, which would result in higher affinity for the more polar epoxide product molecule and water, and promote the secondary ring-opening reaction to produce 1,2-octane diol.

CONCLUDING REMARKS

Modification of **TiSBA15** to produce uncapped titanol sites on a silylated surface (**TiMe**$_{cap}$**SBA15-O**$_2$) yielded a catalyst more active, selective, and efficient for the epoxidation of 1-octene with both anhydrous *tert*-butyl hydroperoxide and aqueous hydrogen peroxide. Subsequent capping of the Ti−OH sites with protic molecules led to two types of catalysts; those modified with phenolate and those modified with carboxylate groups. To our knowledge, this is the first report of heterogeneous titanium epoxidation catalysts possessing fluorinated groups on the surface. Samples modified with phenol groups, $(C_6X_5)_{cap}$**TiMe**$_{cap}$**SBA15** (X = H, F), exhibited marked improvement in catalytic activity (20−50% higher turnovers) and epoxide selectivity (up to 30% higher) with both TBHP and H_2O_2 as oxidants (roughly double the epoxide yield of **TiMe**$_{cap}$**SBA15-O**$_2$). Additionally, with these catalysts, the efficiency of H_2O_2 usage was increased by a factor of 2 to 3 during the course of the catalysis. Samples modified with carboxylic acids, $(CX_3CO)_{cap}$**TiMe**$_{cap}$**SBA15** (X = H, F), exhibited decreased catalytic activity with TBHP (up to 40% lower TON and 10% decrease in epoxide selectivity), but with small improvements in activity when H_2O_2 was used (little change in TON but up to 20% increased epoxide selectivity). These materials; however, were less efficient in the use of H_2O_2 (50% decrease). Thus, carboxylate groups appear to deactivate the titanium centers toward catalytic olefin epoxidation, by changing the structure of the active site and/or by decreasing the hydrophobicity of the surface. Future studies in this area should focus on the development of new molecular precursors incorporating electron-delocalizing and/or electron-withdrawing functionalities (perhaps in place of the isopropoxide ligand in $Ti(O^iPr)[OSi(O^tBu)_3]_3$), which might eliminate the need for multiple surface treatments after synthesis of the catalyst.

The improvement in catalytic activities reported here are comparable to or better than several recently reported for modified, heterogeneous Ti(IV) systems that utilize H_2O_2. Nur and Endud reported nearly a doubling of epoxide yield upon sulfation of the surface of TS-1, and binding of $-OS(O)_2OH$ groups to titanium centers.[66] Post-synthetic silylation of a mesoporous titanosilicate (Ti(IV)-MCM-41) catalyst gave a sample that exhibited an 80% increase in catalytic turnovers and a 20% increase in epoxide selectivity.[79] A supported Ti(IV) catalyst, with a hydrophobic surface, reported by the same authors, displayed smaller gains in catalytic activity (30% increase in turnovers and 10% increase in epoxide selectivity).[79] The latter catalyst also displayed a nearly identical change in catalytic activity when TBHP was used as the oxidant (30% increase in turnovers and 7% increase in epoxide selectivity).

EXPERIMENTAL SECTION

General Procedures. All manipulations were conducted under an inert nitrogen atmosphere using standard Schlenk techniques or a Vacuum Atmospheres drybox, unless otherwise noted. Dry, oxygen-free solvents were used throughout. Benzene-d_6 was purified and dried via vacuum distillation from sodium/potassium alloy.

Toluene and 1-octene were purchased from Aldrich and distilled over sodium prior to use. Phenol was purchased from Fisher Scientific and sublimed prior to use. Pentafluorophenol was purchased from Aldrich and distilled prior to use. *tert*-Butyl hydroperoxide (TBHP, 5.5 M in decane) and $Ti(O^iPr)_4$ were purchased from Aldrich and used as received. Aqueous hydrogen peroxide (30 wt %) was purchased from EM Science and used as received. Tin dichloride hydrate was purchased from Allied Chemical, and used as received. (*N*,*N*-Dimethylamino)trimethylsilane was purchased from Gelest, Inc. and used without further purification. Mesoporous SBA-15,[53] $(^tBuO)_3SiOH$,[84] $Mg(CH_2C_6H_5)_2\cdot 2THF$,[85] and $Ti(OiPr)[OSi(O^tBu)_3]_3$[86] were prepared as reported in the literature, dehydrated under dynamic vacuum, and stored in a vacuum atmospheres drybox until used.

dx.doi.org/10.1021/cs200017s |*ACS Catal.* 2011, 1, 455–467

Synthesis of TiSBA15. A sample of SBA-15 was dried at 120 °C under vacuum for 16 h and handled under a nitrogen atmosphere. A 7.7 g sample of SBA-15 was suspended in hexanes (100 mL). A 40 mL solution of 2.14 g (2.39 mmol) of $Ti(O^iPr)[OSi(O^tBu)_3]_3$ in hexanes was added via cannula at 25 °C under vigorous stirring. The resulting mixture was stirred for 72 h, filtered via cannula, and rinsed with hexanes (3 × 50 mL). The filtered material was dried under vacuum for 2 h at 25 °C and subsequently for 12 h at 120 °C.

Synthesis of Surface Modified TiSBA15 Materials. A 5 g sample of **TiSBA15** was suspended in 50 mL of hexanes. A 20 mL hexanes solution of 8.0 g (45.3 mmol) $Me_2N\text{-}SiMe_3$ (7 equiv based on initial silanol content) was added via cannula at 25 °C, under vigorous stirring. The suspension was stirred for 20 h under a flow of nitrogen. The solid was then filtered via cannula, rinsed with hexanes (3 × 10 mL), dried under vacuum for 12 h at 120 °C, and stored in a drybox. This material is denoted **$TiMe_{cap}SBA15$**. A sample of this material was treated in oxygen at 200 °C for 16 h, dehydrated at 120 °C under vacuum, and stored in a drybox. This material is denoted **$TiMe_{cap}$-SBA15-O_2**.

Titration of Ti−OH Sites in $TiMe_{cap}SBA15\text{-}O_2$. Samples of SBA15 and **$TiMe_{cap}SBA15\text{-}O_2$** were treated using the procedure reported by Lin and Frei.[56] A solution (100 mL) of 0.1 wt % $SnCl_2 \cdot H_2O$ in acetonitrile/dichloromethane (1:1) was added to a 0.2 g sample of catalyst. The solution was stirred for 0.5 h, filtered via cannula, washed with dichloromethane, dried under vacuum at room temperature for 12 h, and stored in a drybox. The resulting materials are designated **Sn-SBA15** and **Sn-$TiMe_{cap}SBA15$**.

Synthesis of $(CX_3CO)_{cap}TiMe_{cap}SBA15$ (X = H, F). A sample of **$TiMe_{cap}SBA15\text{-}O_2$** was suspended in 20 mL of toluene. A toluene solution of CX_3COOH (X = H, F, 5 equiv based on initial silanol content) was added to the suspension via cannula at 25 °C, under vigorous stirring. The suspension was heated at 70 °C and stirred for 24 h under a flow of nitrogen. The solid was then filtered via cannula, rinsed with hexanes (3 × 10 mL), dried under vacuum for 12 h at 120 °C, and stored in a drybox.

Synthesis of $(C_6X_5)_{cap}TiMe_{cap}SBA15$ (X = H, F). A sample of **$TiMe_{cap}SBA15\text{-}O_2$** was suspended in 20 mL of toluene. A toluene solution of C_6X_5OH (X = H, F, 5 equiv based on initial silanol content) was added to the suspension via cannula at 25 °C, under vigorous stirring. The suspension was heated at 70 °C and stirred for 24 h under a flow of nitrogen. The solid was then filtered via cannula, rinsed with hexanes (3 × 10 mL), dried under vacuum for 12 h at 120 °C, and stored in a drybox.

Observation of Titanium-peroxo Intermediates. Samples activated with hydrogen peroxide were prepared by adding 2.0 mL of a 1:1 mixture of acetonitrile and 30 wt % H_2O_2 to 0.050 g of **$TiMe_{cap}$-SBA15-O_2**, **$(CX_3CO)_{cap}TiMe_{cap}SBA15$**, or **$(C_6X_5)_{cap}TiMe_{cap}$-SBA15**. The sample was then heated at 65 °C for 1 h. All volatile materials were removed under vacuum at 25 °C for 16 h, and samples were transferred to a drybox prior to measurement. Reactions of these materials with cyclohexene were conducted by adding 2.0 mL of a 1:1 solution of acetonitrile and cyclohexene and 25 μL of toluene (as an internal standard) to 0.035 g of the material. The suspension was heated at 65 °C for 1 h, and a sample (0.1 mL) was remove, filtered, and analyzed via GC. All volatile materials were removed under vacuum at 25 °C for 16 h, and samples were transferred to a drybox prior to measurement.

Characterization. Solution NMR spectra were recorded at 400 MHz using a Bruker AVB-400 spectrometer (^1H, ^{13}C, ^{19}F). Nitrogen adsorption measurements were measured using a Quantichrome Autosorb 1, and samples were outgassed for 1 h at 120 °C prior to measurement. Infrared spectra were collected using a Thermo Nicolet 6700 FTIR spectrometer. Elemental Analyses were performed by the College of Chemistry microanalytical laboratory at the University of California, Berkeley, Galbraith Laboratories, and Columbia Analytical Services, Inc. DRUV−vis spectra were collected using a Varian-Cary 300 Bio spectrophotometer with a diffuse reflectance attachment. MgO was used as the 100% transmittance standard. Thermal gravimetric analyses were preformed with a Seiko Instruments Inc. EXSTAR 6000 TG/DTA 6300 under a flow of 100 $cm^3\ min^{-1}$ of nitrogen or oxygen and a heating rate of 5 °C min^{-1}. DSC measurements were performed with a TA Instruments DSC 2010 Differential Scanning Calorimeter with a heating rate of 5 °C min^{-1}. Oxygen treatment of materials was conducted using a Lindberg 1200C three-zone furnace with a heating rate of 5 °C min^{-1} under a flow of air or oxygen, with a 4 h isothermal soak. Hydroxyl group content of samples was determined by reaction with $Mg(CH_2C_6H_5)_2 \cdot 2THF$ and quantification of the evolved toluene with ^1H NMR spectroscopy. GC analyses were performed on an HP 6890N system using a phenyl methyl polysiloxane DB-5 capillary column (30.0 m × 320 μm × 1.00 μm), and integration was performed relative to the dodecane internal standard.

Catalytic 1-Octene Epoxidation. A sample of catalyst (0.035 g) was added to a 25 mL round-bottom flask fitted with a reflux condenser and a septum. Under a flow of nitrogen, solvent (5 mL) and 1-octene (1.55 mL) were added via syringe. Dodecane (50 μL) or toluene (25 μL) was added as an internal standard. The mixture was heated to 65 °C where it was allowed to equilibrate for 15 min before the oxidant (1.1 mL TBHP, 5.5 M in decane, or 0.62 mL of H_2O_2, 30 wt % in H_2O) was added via syringe to the rapidly stirring solution. Aliquots (100 μL) were taken from the reaction mixture via syringe, filtered, and cooled. The filtrate was analyzed by gas chromatography (GC), and products were assigned based on known samples analyzed under the same conditions. Additional aliquots (100 μL) were taken to measure residual peroxide concentrations via ^1H NMR spectroscopy. Concentrations were determined via relative peak integration to a dichloromethane internal standard.

■ ASSOCIATED CONTENT

Supporting Information. DRUV−vis spectra for **Sn-SBA15** and **Sn-$TiMe_{cap}SBA15$**, difference of **Sn-$TiMe_{cap}SBA15$** and **Sn-SBA15** DRUV−vis spectra, DRUV−vis spectra of SBA15 samples treated with phenol (C_6H_5OH), pentafluorophenol (C_6F_5OH), acetic acid (CH_3COOH), and trifluoroacetic acid (CF_3COOH), nitrogen adsorption−desorption isotherms, and small-angle X-ray scattering patterns for SBA-15 and all dispersed Ti(IV) catalysts. This material is available free of charge via the Internet at http://pubs.acs.org.

■ AUTHOR INFORMATION

Corresponding Author
*E-mail: tdtilley@berkeley.edu.

■ ACKNOWLEDGMENT

The authors gratefully acknowledge the support of the Director, Office of Energy Research, Office of Basic Energy Sciences, Chemical Sciences division, of the U.S. Department of Energy under contract DE-AC02-05CH11231. We thank A. P. Alivisatos of the University of California, Berkeley for the use of instrumentation (TEM, SAXS).

■ REFERENCES

(1) Sheldon, R. A. *J. Mol. Catal.* **1980**, *7*, 107–126.
(2) Mallat, T.; Baiker, A. *Chem. Rev.* **2004**, *104*, 3037–3058.
(3) Corma, A. *Chem. Rev.* **1997**, *97*, 2373–2419.

(4) Notari, B. In *Advances In Catalysis*; Gates, B. C., Knozinger, H., Eds.; Academic Press: New York, 1996; Vol. 41, pp 253−334.
(5) Ratnasamy, P.; Srinivas, D.; Knözinger, H. In *Advances In Catalysis*; Gates, B. C., Knozinger, H., Eds.; Elsevier Academic Press Inc: San Diego, 2004; Vol. 48, pp 1−169.
(6) Vayssilov, G. N. *Catal. Rev. Sci. Eng.* **1997**, *39*, 209–251.
(7) Sauer, J.-M.; Bao, J.; Smith, R. L.; McClure, T. D.; Mayersohn, M.; Pillai, U.; Cunningham, M. L.; Sipes, I. G. *Drug Metab. Dispos.* **1997**, *25*, 371–378.
(8) van der Schuur, M.; Feijen, J.; Gaymans, R. J. *Polymer* **2005**, *46*, 327–333.
(9) Ding, Y.; Gao, Q.; Li, G.; Zhang, H.; Wang, J.; Yan, L.; Suo, J. *J. Mol. Catal. A: Chem.* **2004**, *218*, 161–170.
(10) Murphy, A.; Stack, T. D. P. *J. Mol. Catal. A: Chem.* **2006**, *251*, 78–88.
(11) Lane, B. S.; Burgess, K. *Chem. Rev.* **2003**, *103*, 2457–2473.
(12) Schaus, S. E.; Brandes, B. D.; Larrow, J. F.; Tokunaga, M.; Hansen, K. B.; Gould, A. E.; Furrow, M. E.; Jacobsen, E. N. *J. Am. Chem. Soc.* **2002**, *124*, 1307–1315.
(13) Corma, A.; Camblor, M. A.; Esteve, P.; Martinez, A.; Perezpariente, J. *J. Catal.* **1994**, *145*, 151–158.
(14) Fujdala, K. L.; Tilley, T. D. *J. Catal.* **2003**, *216*, 265–275.
(15) Tilley, T. D. *J. Mol. Catal. A: Chem.* **2002**, *182*, 17–24.
(16) Ruddy, D. A.; Ohler, N. L.; Bell, A. T.; Tilley, T. D. *J. Catal.* **2006**, *238*, 277–285.
(17) Nozaki, C.; Lugmair, C. G.; Bell, A. T.; Tilley, T. D. *J. Am. Chem. Soc.* **2002**, *124*, 13194–13203.
(18) Lugmair, C. G.; Tilley, T. D. *Monatsh. Chem.* **2006**, *137*, 557–566.
(19) Jarupatrakorn, J.; Tilley, T. D. *J. Am. Chem. Soc.* **2002**, *124*, 8380–8388.
(20) Jarupatrakorn, J.; Coles, M. P.; Tilley, T. D. *Chem. Mater.* **2005**, *17*, 1818–1828.
(21) Holland, A. W.; Li, G. T.; Shahin, A. M.; Long, G. J.; Bell, A. T.; Tilley, T. D. *J. Catal.* **2005**, *235*, 150–163.
(22) Fujdala, K. L.; Drake, I. J.; Bell, A. T.; Tilley, T. D. *J. Am. Chem. Soc.* **2004**, *126*, 10864–10866.
(23) Coles, M. P.; Lugmair, C. G.; Terry, K. W.; Tilley, T. D. *Chem. Mater.* **2000**, *12*, 122–131.
(24) Brutchey, R. L.; Mork, B. V.; Sirbuly, D. J.; Yang, P. D.; Tilley, T. D. *J. Mol. Catal. A: Chem.* **2005**, *238*, 1–12.
(25) Brutchey, R. L.; Lugmair, C. G.; Schebaum, L. O.; Tilley, T. D. *J. Catal.* **2005**, *229*, 72–81.
(26) Brutchey, R. L.; Drake, I. J.; Bell, A. T.; Tilley, T. D. *Chem. Commun* **2005**, 3736–3738.
(27) Larabi, C.; Merle, N.; Norsic, S. b.; Taoufik, M.; Baudouin, A.; Lucas, C.; Thivolle-Cazat, J.; de Mallmann, A.; Basset, J.-M. *Organometallics* **2009**, *28*, 5647–5655.
(28) Rosier, C.; Niccolai, G. P.; Basset, J.-M. *J. Am. Chem. Soc.* **1997**, *119*, 12408–12409.
(29) Bonino, F.; Damin, A.; Ricchiardi, G.; Ricci, M.; Spano, G.; D'Aloisio, R.; Zecchina, A.; Lamberti, C.; Prestipino, C.; Bordiga, S. *J. Phys. Chem. B* **2004**, *108*, 3573–3583.
(30) Salem, I. A.; El-Maazawi, M.; Zaki, A. B. *Int. J. Chem. Kinet.* **2000**, *32*, 643–666.
(31) Tatsumi, T.; Koyano, K. A.; Igarashi, N. *Chem. Commun.* **1998**, 325–326.
(32) Pena, M. L.; Dellarocca, V.; Rey, F.; Corma, A.; Coluccia, S.; Marchese, L. *Microporous Mesoporous Mater.* **2001**, *44*, 345–356.
(33) D'Amore, M. B.; Schwarz, S. *Chem. Commun.* **1999**, 121–122.
(34) Brutchey, R. L.; Ruddy, D. A.; Andersen, L. K.; Tilley, T. D. *Langmuir* **2005**, *21*, 9576–9583.
(35) Fraile, J. M.; Garcia, J. I.; Mayoral, J. A.; Salvatella, L.; Vispe, E.; Brown, D. R.; Fuller, G. *J. Phys. Chem. B* **2003**, *107*, 519–526.
(36) Fraile, J. M.; Garcia, J. I.; Mayoral, J. A.; Vispe, E. *J. Catal.* **2000**, *189*, 40–51.
(37) Ruddy, D. A.; Brutchey, R. L.; Tilley, T. D. *Top. Catal.* **2008**, *48*, 99–106.
(38) Wells, D. H.; Delgass, W. N.; Thomson, K. T. *J. Am. Chem. Soc.* **2004**, *126*, 2956–2962.
(39) Sinclair, P. E.; Carlow, C. R. A. *J. Phys. Chem. B* **1999**, *103*, 1084–1095.
(40) Urakawa, A.; Burgi, T.; Skrabal, P.; Bangerter, F.; Baiker, A. *J. Phys. Chem. B* **2005**, *109*, 2212–2221.
(41) Ikeue, K.; Ikeda, S.; Watanabe, A.; Ohtani, B. *Phys. Chem. Chem. Phys.* **2004**, *6*, 2523–2528.
(42) Lin, W. Y.; Frei, H. *J. Am. Chem. Soc.* **2002**, *124*, 9292–9298.
(43) Berkessel, A.; Adrio, J. A. *J. Am. Chem. Soc.* **2006**, *128*, 13412–13420.
(44) Neurock, M.; Manzer, L. E. *Chem. Commun.* **1996**, 1133–1134.
(45) Kamata, K.; Kuzuya, S.; Uehara, K.; Yamaguchi, S.; Mizuno, N. *Inorg. Chem.* **2007**, *46*, 3768–3774.
(46) Wang, X. Y.; Shi, H. C.; Xu, S. Y. *J. Mol. Catal. A: Chem.* **2003**, *206*, 213–223.
(47) Bordiga, S.; Damin, A.; Bonino, F.; Ricchiardi, G.; Lamberti, C.; Zecchina, A. *Angew. Chem., Int. Ed.* **2002**, *41*, 4734–4737.
(48) Prestipino, C.; Bonino, F.; Usseglio, S.; Damin, A.; Tasso, A.; Clerici, M. G.; Bordiga, S.; D'Acapito, F.; Zecchina, A.; Lamberti, C. *ChemPhysChem* **2004**, *5*, 1799–1804.
(49) Bordiga, S.; Bonino, F.; Damin, A.; Lamberti, C. *Phys. Chem. Chem. Phys.* **2007**, *9*, 4854–4878.
(50) Kholdeeva, O. A.; Trubitsina, T. A.; Maksimovskaya, R. I.; Golovin, A. V.; Neiwert, W. A.; Kolesov, B. A.; López, X.; Poblet, J. M. *Inorg. Chem.* **2004**, *43*, 2284–2292.
(51) Hayashi, K.; Kato, C. N.; Shinohara, A.; Sakai, Y.; Nomiya, K. *J. Mol. Catal. A: Chem.* **2007**, *262*, 30–35.
(52) Fujdala, K. L.; Brutchey, R. L.; Tilley, T. D., . In *Surface and Interfacial Organometallic Chemistry and Catalysis*; Copéret, C., Chaudret, B., Eds.; Springer: Berlin/Heidelberg, 2005; Vol. 16, pp 69−116.
(53) Zhao, D. Y.; Huo, Q. S.; Feng, J. L.; Chmelka, B. F.; Stucky, G. D. *J. Am. Chem. Soc.* **1998**, *120*, 6024–6036.
(54) Fujdala, K. L.; Tilley, T. D. *J. Am. Chem. Soc.* **2001**, *123*, 10133–10134.
(55) Ricchiardi, G.; Damin, A.; Bordiga, S.; Lamberti, C.; Spanò, G.; Rivetti, F.; Zecchina, A. *J. Am. Chem. Soc.* **2001**, *123*, 11409–11419.
(56) Lin, W. Y.; Frei, H. *J. Phys. Chem. B* **2005**, *109*, 4929–4935.
(57) Okamoto, A.; Nakamura, R.; Osawa, H.; Hashimoto, K. *Langmuir* **2008**, *24*, 7011–7017.
(58) Lin, W. Y.; Frei, H. *J. Am. Chem. Soc.* **2005**, *127*, 1610–1611.
(59) Han, H. X.; Frei, H. *Microporous Mesoporous Mater.* **2007**, *103*, 265–272.
(60) Nakamura, R.; Okamoto, A.; Osawa, H.; Irie, H.; Hashimoto, K. *J. Am. Chem. Soc.* **2007**, *129*, 9596–9597.
(61) The experimental procedure was modified as follows: A solution of trifluoroacetic acid (0.3 g) in CH_2Cl_2 (30 mL) was added to 0.1 g of SBA-15 suspended in 20 mL of CH_2Cl_2, in a Teflon-sealed vessel. The suspension was stirred at 70 °C for 24 h. After filtering the solution and drying for 16 h under vacuum at 120 °C, an equivalent DRUV−vis spectrum with similar bands below 300 nm was obtained.
(62) King, R. B.; Kapoor, R. N. *J. Organomet. Chem.* **1968**, *15*, 457–469.
(63) Cannizzo, L. F.; Grubbs, R. H. *J. Org. Chem.* **1985**, *50*, 2316–2323.
(64) Ruddy, D. A.; Tilley, T. D. *J. Am. Chem. Soc.* **2008**, *130*, 11088–11096.
(65) Ruddy, D. A.; Tilley, T. D. *Chem. Commun.* **2007**, 3350–3352.
(66) Nur, H.; Prasetyoko, D.; Ramli, Z.; Endud, S. *Catal. Commun.* **2004**, *5*, 725–728.
(67) Marchese, L.; Maschmeyer, T.; Gianotti, E.; Coluccia, S.; Thomas, J. M. *J. Phys. Chem. B* **1997**, *101*, 8836–8838.
(68) Klein, S.; Weckhuysen, B. M.; Martens, J. A.; Maier, W. F.; Jacobs, P. A. *J. Catal.* **1996**, *163*, 489–491.
(69) LeNoc, L.; On, D. T.; Solomykina, S.; Echchahed, B.; Beland, F.; Moulin, C. C. D.; Bonneviot, L. *Stud. Surf. Sci. Catal.* **1996**, *101*, 611–620.
(70) Shetti, V. N.; Manikandan, P.; Srinivas, D.; Ratnasamy, P. *J. Catal.* **2003**, *216*, 461–467.

(71) Mimoun, H.; Postel, M.; Casabianca, F.; Fischer, J.; Mitschler, A. *Inorg. Chem.* **1982**, *21*, 1303–1306.
(72) Kholdeeva, O. A.; Maksimov, G. M.; Maksimovskaya, R. I.; Kovaleva, L. A.; Fedotov, M. A.; Grigoriev, V. A.; Hill, C. L. *Inorg. Chem.* **2000**, *39*, 3828–3837.
(73) Postel, M.; Casabianca, F.; Gauffreteau, Y.; Fischer, J. *Inorg. Chim. Acta* **1986**, *113*, 173–180.
(74) Sakai, Y.; Kitakoga, Y.; Hayashi, K.; Yoza, K.; Nomiya, K. *Eur. J. Inorg. Chem.* **2004**, *2004*, 4646–4652.
(75) Yudanov, I. V.; Gisdakis, P.; Di Valentin, C.; Rösch, N. *Eur. J. Inorg. Chem.* **1999**, *1999*, 2135–2145.
(76) Romão, C. C.; Kuhn, F. E.; Herrmann, W. A. *Chem. Rev.* **1997**, *97*, 3197–3246.
(77) Gao, F.; Yamase, T.; Suzuki, H. *J. Mol. Catal. A: Chem.* **2002**, *180*, 97–108.
(78) Jimtaisong, A.; Luck, R. L. *Inorg. Chem.* **2006**, *45*, 10391–10402.
(79) Lin, K. F.; Wang, L. F.; Meng, F. Y.; Sun, Z. H.; Yang, Q.; Cui, Y. M.; Jiang, D. Z.; Xiao, F. S. *J. Catal.* **2005**, *235*, 423–427.
(80) Corma, A.; Domine, M.; Gaona, J. A.; Jorda, J. L.; Navarro, M. T.; Rey, F.; Perez-Pariente, J.; Tsuji, J.; McCulloch, B.; Nemeth, L. T. *Chem. Commun.* **1998**, 2211–2212.
(81) Morlanés, N.; Notestein, J. M. *J. Catal.* **2010**, *275*, 191–201.
(82) Notestein, J. M.; Andrini, L. R.; Kalchenko, V. I.; Requejo, F. G.; Katz, A.; Iglesia, E. *J. Am. Chem. Soc.* **2007**, *129*, 1122–1131.
(83) Coffindaffer, T. W.; Steffy, B. D.; Rothwell, I. P.; Folting, K.; Huffman, J. C.; Streib, W. E. *J. Am. Chem. Soc.* **1989**, *111*, 4742–4749.
(84) Abe, Y.; Kijima, I. *Bull. Chem. Soc. Jpn.* **1969**, *42*, 1118–1123.
(85) Dryden, N. H.; Legzdins, P.; Rettig, S. J.; Veltheer, J. E. *Organometallics* **1992**, *11*, 2583–2590.
(86) Gunji, T.; Kasahara, T.; Abe, Y. *J. Sol-Gel Sci. Technol.* **1998**, *13*, 975–979.